ELSEVIER

Journal of Power Sources 107 (2002) 192–200

JOURNAL OF POWER SOURCES

www.elsevier.com/locate/jpowsour

Micro-structural design and function of an improved absorptive glass mat (AGM) separator for valve-regulated lead–acid batteries

Y. Nakayama[a,*], K. Kishimoto[a], S. Sugiyama[b], S. Sakaguchi[b]

[a]*Yuasa Corporation, 2-3-21 Kosobe-cho, Takatsuki, Osakga 569-1115, Japan*

[b]*Nippon Sheet Glass Co. Ltd., NGF Company, 4902, Komoricho, Takachaya, Tsu, Mie 514-0817, Japan*

Received 22 August 2001; accepted 10 October 2001

Abstract

Two important properties of absorptive glass mat (AGM) separators are examined in order to design optimum separators for advanced valve-regulated lead–acid (VRLA) batteries. Acid stratification in the separator depends on its micro-glass-fibre diameter, and it is found that the extent of stratification can be estimated based on hydrodynamics theory. Decreasing the plate-group pressure of the separator in the wetted state is also investigated, and it is considered that the phenomenon is caused by the balance between the fibre strength and the surface tension of acid solution. Given these results, the way to design AGM separators according to purpose has been identified. Accordingly, a new AGM separator has been developed and this functions both to suppress stratification and to maintain plate-group pressure.

Keywords: Absorptive glass mat; Acid-dripping speed; Plate-group pressure; Separator; Stratification; Valve-regulated lead–acid battery

1. Introduction

The lead–acid battery has been used widely as a secondary battery for 140 years, since its invention by Planté in 1859 [1]. Development of the battery has been pursued vigorously all over the world. The valve-regulated lead–acid (VRLA) battery is a more recent variant that generally uses an absorptive glass mat (AGM) separator. The market for VRLA batteries has been growing for telecommunications [2,3] and motor-cycle [4,5] use. Moreover, the advanced VRLA battery has lately attracted considerable attention for future automobiles [6–9].

The AGM separator is an important component of VRLA batteries, but the function of present materials is far from ideal. There are three main requirements of the AGM separator for improving the performance of the VRLA battery. The first is to prevent a short-circuit between the positive and the negative plates. This is the most important and basic function of the separator.

The second function is to retain the sulfuric acid electrolyte reliably, that is, to maintain the amount and the concentration of the electrolyte uniformly throughout the separator. The difference in acid concentration, which often occurs between the upper and the lower parts of the batteries, is called 'stratification' [10]. Acid stratification in the AGM separator is a serious issue for VRLA batteries. Stratification is closely related to sulfation which is a major failure mode of the negative plate of lead–acid batteries [11,12]. Therefore, suppressing the stratification occurring in the AGM separator would make it possible to extend the life performance of the batteries.

The third function is that the AGM separator should maintain its elasticity in order to keep a good contact force between itself and the plates of electrodes, even when it absorbs the electrolyte. In this paper, such elasticity of the AGM separator is called the 'wet-elasticity'. The wet-elasticity is a very important property which ensures the supply of acid to the plates and maintains the ionic conductivity, regardless of the amount of electrolyte retained within the separator. Furthermore, it has been shown [13–17] that the plate-group pressure caused by the elasticity is strongly effective in suppressing the capacity loss of the positive plate during deep cycling. Hence, management of the wet-elasticity of the separator has a great impact on the improvement of the performance of the VRLA battery.

In this paper, we present an experimental technique to evaluate the second and the third functions of the AGM separator, and we discuss the data obtained in terms of a physical model.

* Corresponding author. Tel.: +81-726-85-2681; fax: +81-726-75-3070.
E-mail address: yasuhide_nakayama@yuasa-jpn.co.jp (Y. Nakayama).

0378-7753/02/$ – see front matter
PII: S0378-7753(01)01005-9

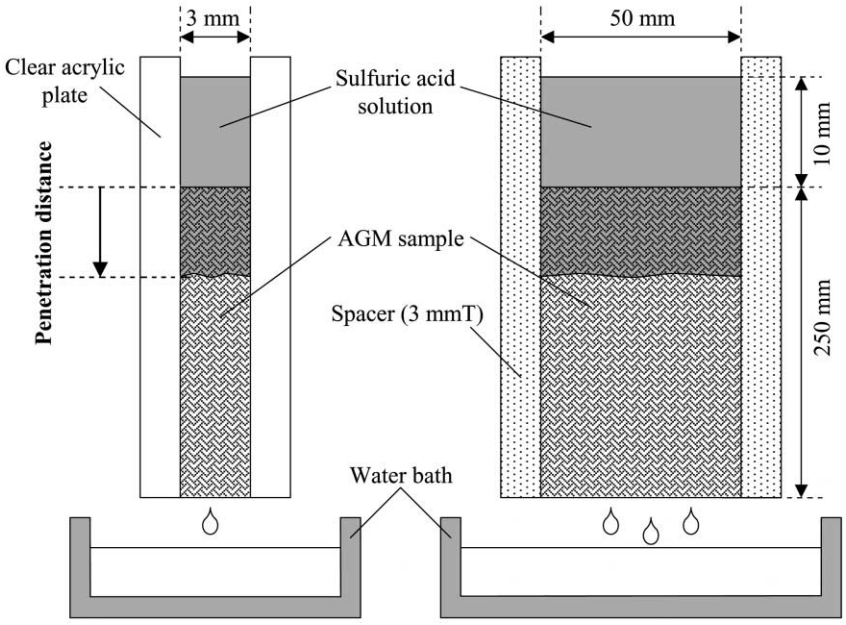

Fig. 1. Schematic of the cell for acid-dripping speed measurement.

2. Experimental

2.1. Measurement of acid-dripping speed

Since it was considered that there is correlation between the stratification in the AGM separator and the acid-dripping speed through the separator, the following study was carried out to evaluate stratification.

The experiment was performed using the cell shown schematically in Fig. 1. An AGM specimen of 100 cm^2 was obtained by cutting a sample from a separator to be examined, and its pressed density (P_d) was recorded with the thickness in a state compressed by a load of 50.0 kg dm^{-2}.

Another AGM sample of 250 mm × 50 mm, which is the size necessary for the examination, was prepared from the same separator and was adjusted on a packing mass (P_m). It is a mass for which the compressed state of the sample in the cell is 50.0 kg dm^{-2}, and it is given by:

$$P_m\,(g) = 250\,(mm) \times 50\,(mm) \times 3\,(mm) \times P_d\,(g\,cm^{-3}) \times 10^{-3} \quad (1)$$

The AGM sample was immersed in water held at 20 ± 3 °C. After removal of excess water, the wetted sample was assembled into a cell. Sulfuric acid solution with a concentration of 1.30 g cm^{-3} at 20 ± 3 °C was coloured by methyl-orange, and then it was added gently to a level of 100 mm above the sample. This acid level was maintained throughout the experiment by adding acid as necessary. The time was counted from the moment when the acid filling was finished, and the penetration distance of the acid from the top of the sample was measured at 5, 10, 30, and 60 min, respectively.

2.2. Measurement of wet-elasticity

The wet-elasticity of the AGM separator was measured by the following procedure using the testing equipment shown schematically in Fig. 2.

Some sheets of AGM sample of 100 mm^2 were obtained by cutting the separator to be examined and they were stacked to be between 5.5 and 7.5 mm in thickness. The stacks were used as the test samples for the equipment. A sulfuric acid solution with a concentration of 1.30 g cm^{-3} at 20 ± 3 °C was prepared for the following experiments.

Before the main experiment for the wet-elasticity, a preliminary test was performed as follows. A test sample was put into a vinyl bag. The sample was placed in the equipment and then compressed with a turn handle until a pressure of 40.0 kg dm^{-2} was detected by a load cell. After that, acid at 20 ± 3 °C was poured on to the sample unto acid seeped from the side of the sample. The total volume of acid absorbed by the sample was measured and this was assumed to be the acid saturation point (P_2) of the AGM sample.

The following main experiment was then carried out. Another AGM sample in a vinyl bag was set into the equipment and compressed to 40.0 kg dm^{-2}. The pressure was reset 5 times at intervals of 1 min to 40.0 kg dm^{-2}, because it decreased with time. About 10 g of acid at 20 ± 3 °C was poured on to the sample. The pressure of the sample in the wet condition was recorded 2 min after the pouring. This acid pouring and pressure measurement was repeated until the total poured amount came to $P_2 - 20$ g, (the pourings were done at intervals of 3 min). Then, the pouring amount was changed to 5 g, and the

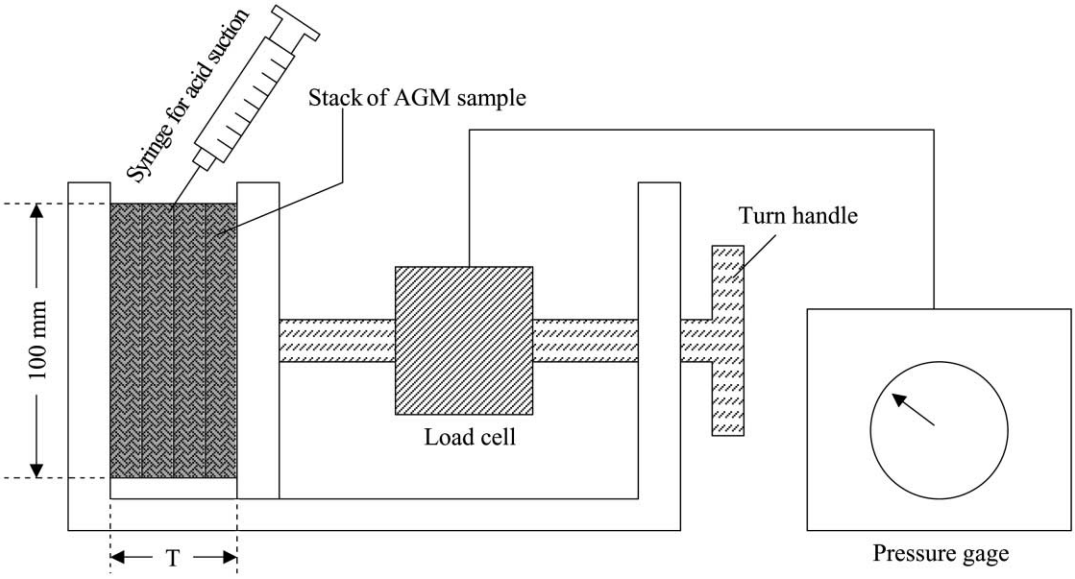

Fig. 2. Schematic of equipment for wet-elasticity measurement.

pressure measurement was made 2 min after the pouring. The acid pouring and pressure measurement was repeated until the acid seeped from the side of the sample.

After the saturation was complete, the acid absorbed within the AGM sample was sucked up using a syringe for the pressure change to become approximately 2 kg dm^{-2}. At that time, the amount of acid sucked was measured. The pressure of the sample was also recorded 2 min after the suction. The acid suction and pressure measurement were repeated until the pressure no longer changed.

Although, the procedure detailed above was for an experiment that used sulfuric acid solution of 1.30 g cm^{-3}, the wet-elasticity of the AGM separator can be also examined using other solutions which include pure water, sulfuric acid of different concentration, and sulfuric acid with some surfactant.

3. Results

3.1. Acid-dripping speed

The penetration distances of the acid with time for two AGM samples made of micro-glass-fibre of 0.7 or 1.5 μm diameter (Φ) are shown in Fig. 3. Since the penetration rates are almost linear with time, regardless of their fibre composition, we used the penetration distance at 60 min as the acid-dripping speed (mm h^{-1}) of the sample.

The acid-dripping speeds of AGM samples made of a variety of different fibre diameters are listed in Table 1. These data are reproduced as a graph in Fig. 4. By means of this experiment, it is established that the acid-dripping speed depends on the fibre diameter of the AGM. The speed is faster when the diameter is larger.

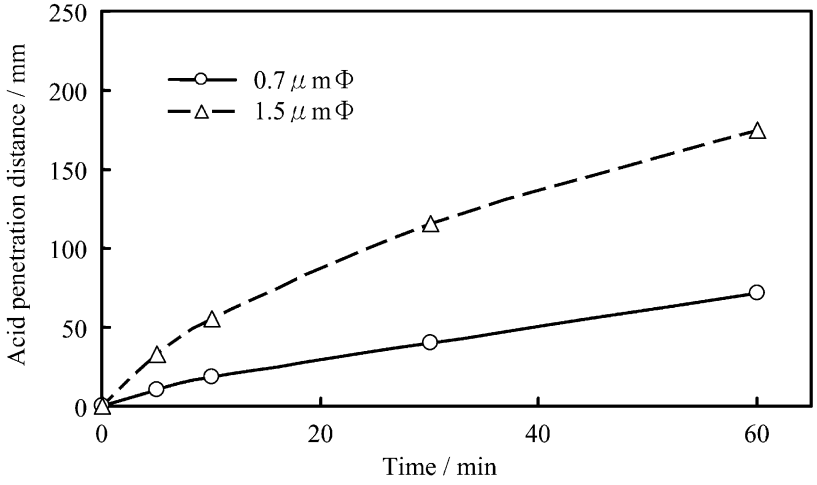

Fig. 3. Acid penetration (dripping) distance with time for different AGM samples.

Table 1
Acid-dripping speed of AGM samples with different fibre diameters

Fibre diameter (μm)	Acid-dripping speed (mm h^{-1})
0.5	29
0.6	49
0.7	71
0.8	91
1.5	175
2.5	>250
4.0	>250

The results for three AGM samples made of blended fibres are shown in Table 2, together with the composition of the fibres. It is found that the acid-dripping speed is faster when a larger amount of coarse fibres are blended into the AGM separator.

3.2. Wet-elasticity

The change in wet-elasticity of an AGM sample consisting of blended fibres (60% 0.6 μmΦ and 40% 0.8 μmΦ) with the degree of acid saturation in the sample is shown in Fig. 5. For this experiment, 1.30 g cm^{-3} sulfuric acid was used. In Fig. 5, P_0 shows the initial elasticity, which was controlled at 40.0 kg dm^{-2}, with the sample dry. It is found that the wet-elasticity gradually decreases until 13.0 kg dm^{-2}, which is indicated at the minimum point P_1, with acid pouring. The degree of acid saturation at P_1 is approximately 76%. The wet-elasticity increases with pouring and becomes approximately constant from 21.0 kg cm^{-2} (point P_2). In the case of

Table 2
Acid-dripping speed of three AGM samples made of different glass-fibre compositions

Fibre diameter (μm)	Sample		
	A	B	C
0.6	60%	30%	45%
0.8	40%	50%	–
2.5	–	20%	–
4.0	–	–	55%
Acid-dripping speed (mm h^{-1})	66	115	105

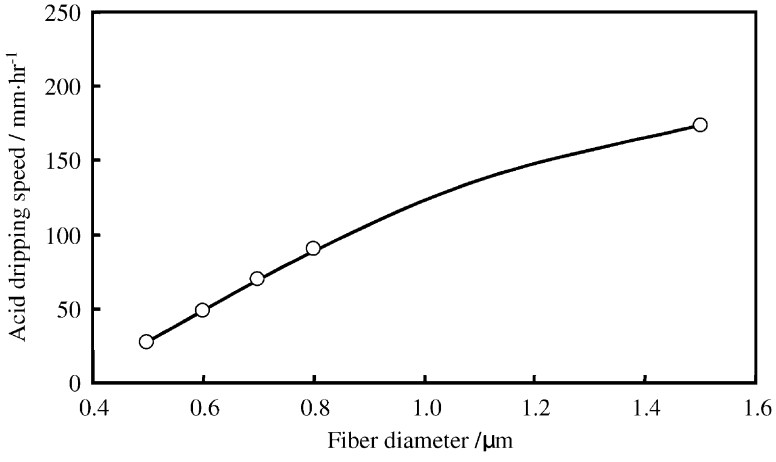

Fig. 4. Relation between fibre diameter and acid-dripping speed of AGM samples.

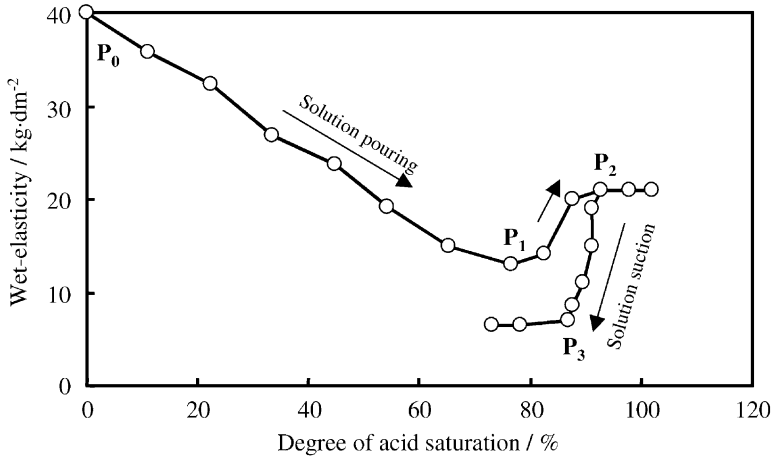

Fig. 5. Wet-elasticity change of AGM sample during solution pouring and suction. AGM: 0.6 μmΦ (60%) + 0.8 μmΦ (40%). Solution: 1.30 g cm^{-3} sulfuric acid.

Table 3
Wet-elasticity of AGM samples with different fibre diameters[a]

Fibre diameter (μm)	P_1	P_2	P_3
0.5	11.2	26.3	4.2
0.6	11.2	23.0	4.2
0.7	15.0	24.2	7.9
0.8	19.4	25.1	11.3
1.5	24.2	29.5	16.5
2.5	25.1	28.6	17.7
4.0	30.9	31.6	23.6

[a] Points P_1, P_2 and P_3 (kg dm^{-2}), see Fig. 5. Solution: 1.30 g cm^{-3} sulfuric acid.

acid suction, however, the wet-elasticity decreases drastically to 6.5 kg dm^{-2} (point P_3). This change never traces back on the P_2–P_1–P_0 line.

The P_1, P_2 and P_3 points in the wet-elasticity change of the AGM samples made of different fibre diameters are listed in Table 3. The wet-elasticity changes of the samples made of the 0.8 or 4.0 μmΦ fibre are also shown in Fig. 6. The solution used for these experiments was 1.30 g cm^{-3} sulfuric acid. From the results, it is found that the wet-elasticity change during the acid pouring followed by suction varies with the difference in the fibre diameters in the AGM. Namely, decrease in the wet-elasticity is suppressed if the AGM is composed of coarser fibres.

The change in wet-elasticity was also measured during pouring pure water on an AGM sample which consisted of the blended fibres, 60% 0.6 μmΦ and 40% 0.8 μmΦ. The result is shown in Fig. 7, for 1.30 g cm^{-3} sulfuric acid pouring. To investigate the influence of the surface tension of the solution, the wet-elasticity change of the same AGM was measured using 1.30 g cm^{-3} sulfuric acid solutions with 0.1 wt.% surfactant (Unidyne). The result is shown in Fig. 8. The wet-elasticity change of the AGM is less variable, even if the concentration of the solution is different (Fig. 7). It is confirmed, however, that the surface tension of the solution influences the change in wet-elasticity (Fig. 8).

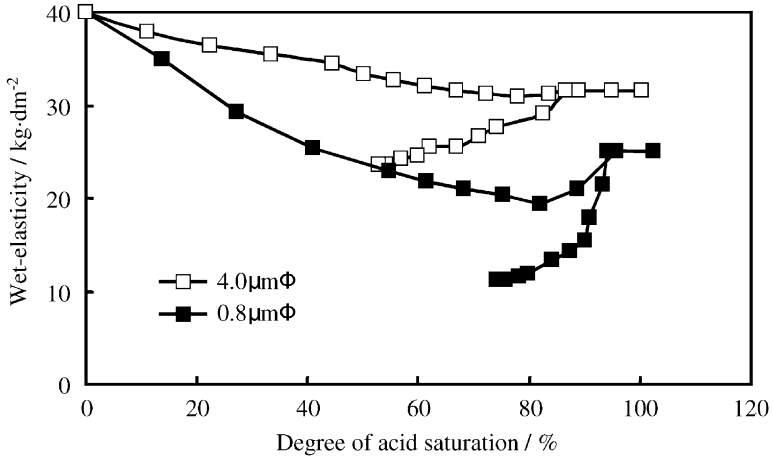

Fig. 6. Influence of fibre diameter of AGM on wet-elasticity. Solution: 1.30 g cm^{-3} sulfuric acid.

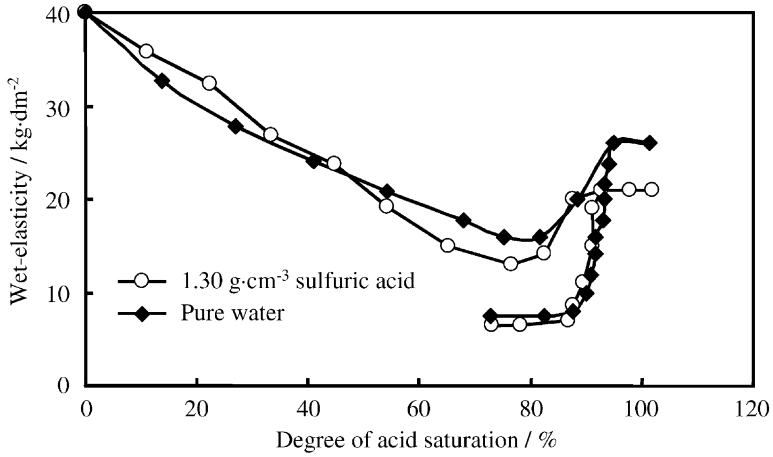

Fig. 7. Influence of acid concentration on wet-elasticity of AGM. AGM: 0.6 μmΦ (60%) + 0.8 μmΦ (40%).

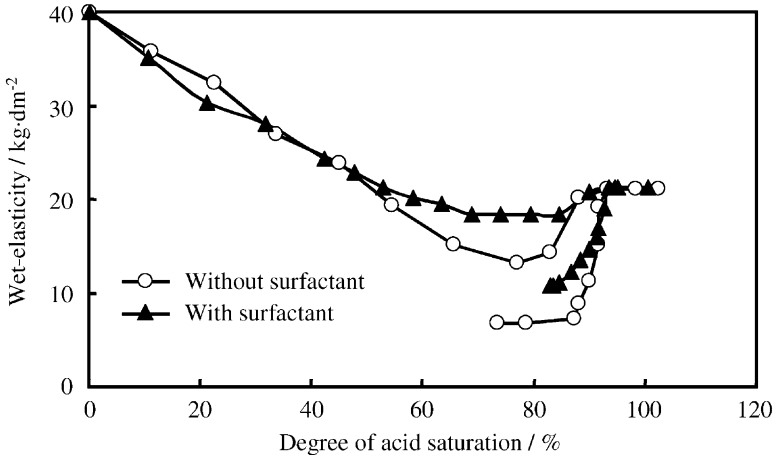

Fig. 8. Influence of surface tension of solution on wet-elasticity of AGM. AGM: 0.6 μmΦ (60%) + 0.8 μmΦ (40%). Solution: 1.30 g cm^{-3} sulfuric acid with or without 0.1% surfactant (Unidyne).

4. Discussion

4.1. Acid-dripping speed and microstructure of AGM

In order to understand the relation between the acid-dripping speed and the microstructure of the AGM separator, the experimental system is expressed as the model shown in Fig. 9. In this model, it can be considered that two solutions, with different viscosity of η_1 and η_2, are flowing with velocity Q through an imaginary tube of radius r. The following equation for the velocity (Q) of the flowing solution is derived using the Hagen–Poiseuille law.

$$Q = \frac{\pi r^4 (P_1 - P_2)}{8\eta L} \tag{2}$$

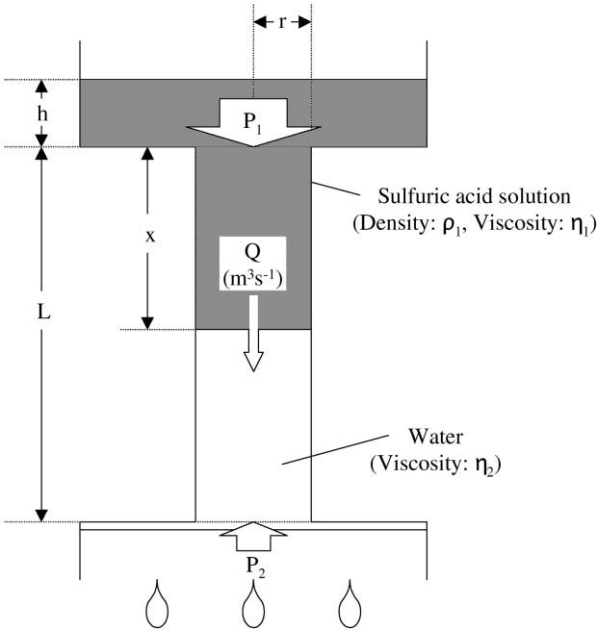

Fig. 9. Simplified model of experimental system for acid-dripping speed measurement.

where Q is the velocity of flowing solution (m^3 s^{-1}), r the radius of tube (m), P_1 the pressure by head acid $= \rho_1 gh$ (Pa), P_2 the pressure by surface tension of solutions (Pa), $P_1 - P_2$ the pressure difference (Pa), L the length of tube (m), and η the average viscosity of acid and water at x (Pa s).

Since η is the average viscosity of the acid and water when an interface line exists between them at x, η is given by:

$$\eta = \frac{\eta_1 x + (L - x)\eta_2}{L} \tag{3}$$

Therefore, Eq. (2) can be modified as follows:

$$Q = \frac{\pi r^4 (P_1 - P_2)}{8[(\eta_1 - \eta_2)x + L\eta_2]} \tag{4}$$

Thus, Eq. (4) can be divided by πr^2 which is the cross-sectional area of the tube, so that the next differential equation is given as below.

$$V = \frac{\mathrm{d}x}{\mathrm{d}t} = \frac{r^2 (P_1 - P_2)}{8[(\eta_1 - \eta_2)x + L\eta_2]} \tag{5}$$

where V represents the velocity of the interface line at x (m s^{-1}). Moreover, the radius r of imaginary tube is expressed in Eq. (6) using a coefficient K, which can be called the microstructure coefficient of the separator, i.e.

$$r = Kd \tag{6}$$

where d is the diameter of micro-glass-fibre of AGM separator (m).

By solving Eq. (5) using $r = Kd$, the equations give K in terms of the measured data, t, d and x, i.e.

$$K^2 t = \frac{4(\eta_1 - \eta_2)x^2 + 8L\eta_2 x}{d^2 (P_1 - P_2)} \tag{7}$$

and

$$x = \frac{-2L\eta_2 + [4L^2\eta_2^2 + K^2 d^2 (P_1 - P_2)(\eta_1 - \eta_2)t]^{1/2}}{2(\eta_1 - \eta_2)} \tag{8}$$

Table 4
Microstructure coefficient K of AGM samples with different fibre diameters

Fibre diameter (μm)	0.5	0.6	0.7	0.8	1.5	2.5	4.0
K	7.75	8.76	9.34	9.61	7.84	6.87	5.98

The values of the microstructure coefficient K which were computed by experimental data are given in Table 4 and as a graph in Fig. 10. From these results, it is found that the values of K change with fibre diameter, though K is expressed as a proportional coefficient of the diameter in Eq. (6). An interesting behaviour of K is found in this figure. Namely, the value of K shows a peak at 0.8 μmΦ, but K decreases drastically in the region of $d < 0.8$ μmΦ and it decreases steadily in the region of $d > 0.8$ μmΦ.

In the region of $d > 0.8$ μmΦ, it is considered that turbulence occurs in the flow of solution because the flowing speed is fast. Therefore, the steady decrease in K is caused by a resistance which is generated by the turbulent flow. The behaviour of K in the region of $d < 0.8$ μmΦ, however, cannot be explained for the same reason. A strong interaction may exist between the fibre and the solution in this region, because the distance between the fibres is too narrow. Yet, making the AGM separator from fibre of 0.5 or 0.6 μmΦ would be more effective in reducing the acid-dripping speed, and thereby in suppressing stratification in the separator, because the K value is smaller than that of 0.8 μmΦ. We also suggest that such considerations are important in the design of new AGM separators made of fibres of different diameters.

4.2. A model for wet-elasticity change

To explain why the wet-elasticity change occurs during pouring and suction of the sulfuric acid solution, we have considered a model which consists of the elasticity of glass-fibres and the surface tension of the solution. This is shown in Fig. 11.

Drawing (1) is a schematic of the microstructure of an AGM separator in the dried state, without compression. There are four fixed points where the fibres cross each other because a friction force is generated between the fibres at these points. The structure and the restitutive forces (F_{P0}) when the separator is compressed are shown in drawing (2), which corresponds to the state of the separator at P_0 in Fig. 5. Since F_{P0} is the force caused by the deformation of the glass-fibre, its value per unit length of fibre becomes larger when the fibre diameter is larger.

Drawings (3)–(5) explain the changes in the structure and the restitutive forces during solution pouring, and they correspond to the P_0–P_1 line in Fig. 5. When the sulfuric acid solution is poured, the solution bridges between the fibres, as shown in the drawings. At this stage, the surface tension at each surface of the solution works to pull the fibres inwards; F_{st} in Fig. 11 represents the force generated by this surface tension. Therefore, the restitutive force decreases with solution pouring because the amount of solution surface increases, as shown in the drawings. Such decrease of the restitutive force of each fibre would cause the decrease in the wet-elasticity of the AGM separator up to P_1 in Fig. 5.

When the solution was poured beyond the point P_1, the amount of solution surface begins to decrease, as shown in drawing (6). Therefore, the restitutive force F_4 at that time becomes bigger than F_3 at P_1. The solution begins to penetrate into the crossing points of fibres, and then it lubricates between the fibres. As a result, the crossing points penetrated by the solution can no longer fix the fibres.

At last, the space made by the fibres is filled up with the solution, as shown in drawing (7). The restitutive force F_5 at this stage is less than F_0, because the fibres can move comparatively freely. It is considered that such a state corresponds to P_2 in Fig. 5.

Drawing (8) shows the state when the solution is sucked up after P_2. Since the surfaces of solution again appear with a decrease of the solution, the fibres are pulled and are moved to the inside by the surface tension F_{st}. Consequently, the distance between the fibres decreases, so that the total

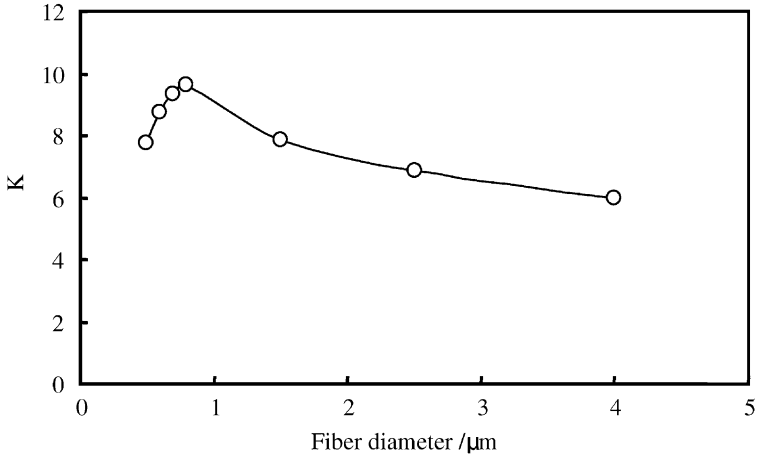

Fig. 10. Relation between microstructure coefficient K and micro-glass-fibre diameter.

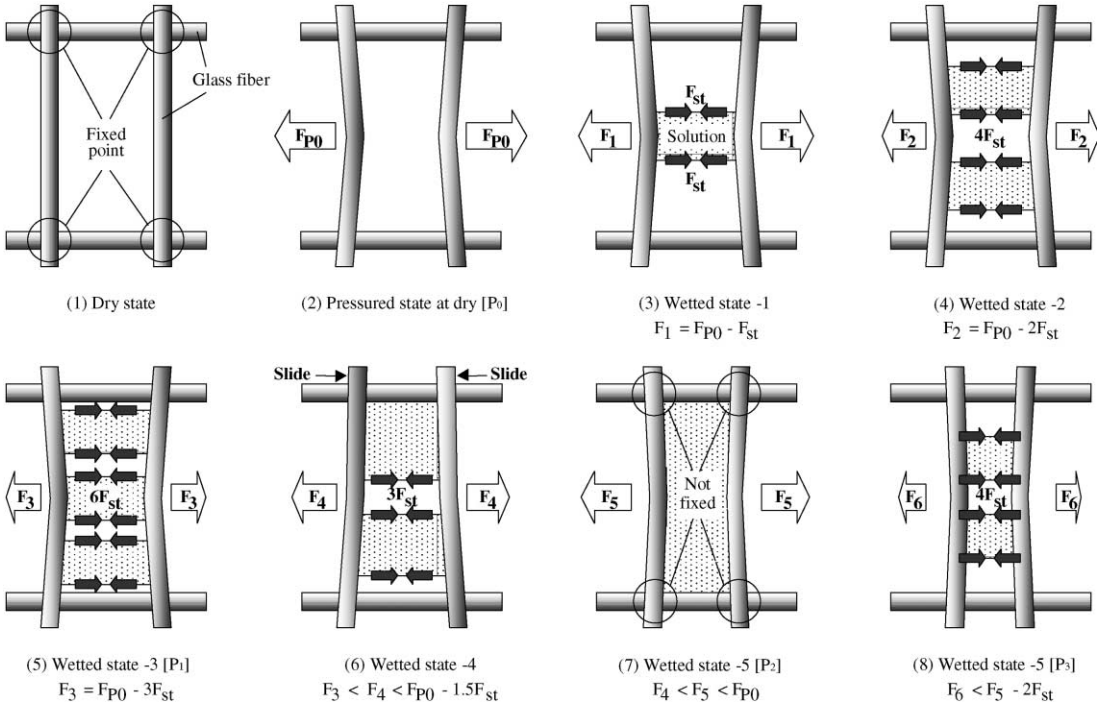

Fig. 11. Model of wet-elasticity change during solution pouring and suction.

Table 5
Properties of new AGM separator

Composition of fibres (wt.%)		Properties			
0.6 μmΦ	4.0 μmΦ	Acid-dripping speed (mm h^{-1})	Wet-elasticity (kg dm^{-2})		
			P_1	P_2	P_3
45	55	105	21.8	26.3	15.3

volume of the AGM separator is reduced. It is considered that such a phenomenon causes a drastic decrease in the wet-elasticity change to P_3 without tracing back on the P_2–P_1–P_0 line.

From this consideration, the coarser fibre is a more effective means to suppress the decrease of the wet-elasticity change, because its restitutive force is larger and the contacting area is wider than for fine fibres.

4.3. Performance of blended AGM separator

The fibre diameter which is optimum for suppression of stratification and that which gives improvement of the wet-elasticity are in conflict. Therefore, we have attempted to make a suitable separator by blending fibres that have different diameters in order to solve the conflict of properties.

As an example of the results, each property of a newly developed AGM separator is shown in Table 5. This separator consists of blended fibres of 45% 0.6 μmΦ and 55% 4.0 μmΦ. From these data, we can estimate that the separator has an acid-dripping speed of the 0.9 μmΦ class and a wet-elasticity of the 1.4 μmΦ class. In this way, it is possible to develop a new AGM separator that has excellent prospects for improving the performance of VRLA batteries.

5. Conclusions

We have evaluated the acid-dripping speed and the wet-elasticity using AGM separators that have different fibre diameters. The experimental results have led to the following conclusion.

1. The acid-dripping speed depends completely on the glass-fibre diameter of the AGM. Therefore, the stratification phenomenon can be suppressed by using a separator which is composed of fine fibres.
2. The microstructure coefficient K has been calculated using the Hagen–Poiseuille law. The behaviour of K shows that an AGM separator using fibre of 0.5 or 0.6 μmΦ is more effective in suppressing stratification in the separator.

3. Sufficient wet-elasticity of an AGM separator to maintain the plate-group pressure becomes less when the separator is composed of fine fibres.
4. The wet-elasticity change, which occurs during pouring and suction of sulfuric acid solution, is explained in terms of the balance between the fibre strength and the surface tension of the solution.
5. A newly developed separator, which consists of blended fibres that are 45% 0.6 μmΦ and 55% 4.0 μmΦ has an acid-dripping speed equivalent to the 0.9 μmΦ class and a wet-elasticity equivalent to the 1.4 μmΦ class. This result means that the conflicting properties of the AGM separator can be solved by blending fibres.

Through this study, we have obtained a guideline for suppressing stratification while maintaining plate-group pressure. The requirements for AGM separators for VRLA batteries, however, have been steadily increasing. In particular, developing a thinner AGM separator, which prevents short-circuits, has become a most important issue, because this is a key technology to realize the higher power 36 V VRLA battery for mild hybrid vehicles. Therefore, we are developing a novel AGM separator for advanced VRLA batteries by applying the analysis presented here.

Acknowledgements

We express our sincere thanks to Mr. Junji Muto, ex-chief engineer, and Mr. Hironori Kitawaki, ex-associate chief engineer, of Nippon Sheet Glass Co. Ltd. for their great cooperation.

References

[1] G. Planté, Recherches sur l'Électricité, Gauthier-Villars, Paris, 1883, p. 30.
[2] Y. Matsuyama, M. Sasaki, Yuasa-Jiho 87, (1999) 17–21, in Japanese.
[3] D.C. Pierce, S. Sasabe, K. Sato, Y. Matsuyama, Proceedings of INTELEC 2000, Phoenix, September 2000, pp. 34–36.
[4] E. Kato, S. Tanaka, J. Power Sources 88 (1) (2000) 98–100.
[5] Y. Iwaguchi, Y. Kawamoto, N. Yamada, K. Kawakita, S. Tanaka, Yuasa-Jiho 89 (2000) 10–13, in Japanese.
[6] Y. Nakayama, in: Proceedings of the first presentation on Advanced Automotive Battery Conference, Las Vegas, February 2001.
[7] M. Shiomi, in: Proceedings of the Battery Council International Annual Convention, Las Vegas, May 2001.
[8] F. Trinidad, F. Sáez, J. Valenciano, J. Power Sources 95 (1–2) (2001) 24–37.
[9] P. Lailler, J.-F. Sarrau, C. Sarrazin, J. Power Sources 95 (1–2) (2001) 58–67.
[10] H. Tuphorn, J. Power Sources 31 (1990) 57–67.
[11] B. Culpin, D.A.J. Rand, J. Power Sources 36 (1991) 415–438.
[12] K. Hirakawa, S. Takahashi, M. Morimitsu, Y. Yamaguchi, Y. Nakayama, Yuasa-Jiho 87, (1999) 42–46, in Japanese.
[13] K.K. Constanti, A.F. Hollenkamp, M.J. Koop, K. McGregor, J. Power Sources 55 (2) (1995) 269–275.
[14] K. Peters, J. Power Sources 59 (1–2) (1996) 9–13.
[15] P.T. Moseley, in: Proceedings of the Battery Council International Annual Convention, San Diego, April 1997.
[16] K. McGregor, A.F. Hollenkamp, M. Barber, T.D. Huynh, H. Ozgun, C.G. Phyland, A.J. Urban, D.G. Vella, L.H. Vu, J. Power Sources 73 (1) (1998) 65–73.
[17] K. Sawai, M. Shiomi, Y. Okada, K. Nakamura, M. Tsubota, J. Power Sources 78 (12) (1999) 46–53.